Effects of strain on island morphology and size distribution in irreversible submonolayer growth

Giridhar Nandipati and Jacques G. Amar
Department of Physics and Astronomy, University of Toledo, Toledo, Ohio 43606, USA
(Received 16 September 2005; revised manuscript received 21 November 2005; published 12 January 2006)

The effects of strain on the island morphology and size distribution in irreversible submonolayer growth with rapid island relaxation are investigated. In our simulations the strain energy is approximated by an isotropic $1/r^3$ interaction. While the island density increases with strain, in the presence of sufficient island relaxation due to edge diffusion, the island shape changes from square to rectangular. However, due to fluctuations, there is a broad distribution of island widths. General scaling forms for the island width and island-length distributions are derived and good scaling is obtained as a function of coverage while there is only a relatively weak dependence on the strain. The scaled island-size distribution is also found to be only weakly affected by strain. These latter results are in qualitative agreement with recent experimental results for InAs/GaAs(100) growth.

DOI: 10.1103/PhysRevB.73.045409 PACS number(s): 81.15.Aa, 68.55.−a, 81.10.Aj

I. INTRODUCTION

Heteroepitaxial growth is an important process[1–3] for the fabrication of nanostructures ranging from quantum wires[4] to quantum dots.[5] In many cases, the existence of strain due to lattice mismatch can lead to the formation of three-dimensional (3D) clusters,[6,7] whose shape can depend on a variety of factors. A classic example of such 3D clusters are the (105)-facet "hut" clusters observed in growth of Si/Ge(001). By analyzing the strain energy of a 3D island with a rectangular base, Tersoff and Tromp[8] have investigated the effects of biaxial strain on the equilibrium shape and aspect ratio of dislocation-free 3D islands. In particular, they demonstrated the existence of a shape transition such that for islands smaller than a critical size the islands are "square," while for larger sizes the islands are elongated with a selected width which is determined by the competition between the strain and surface energies. In more recent work[9,10] the effects of anisotropic strain on the equilibrium shape of 2D islands have also been studied.

While there have been extensive studies of the effects of strain on the equilibrium shape of 2D and 3D islands, there has been less work on the effects of strain on the island-shape during growth. Recently, Steinbrecher *et al.*[12] have studied the effects of strain on the fractal growth of individual islands in the absence of island relaxation. In their model, the elastic interaction was approximated by a $1/r^3$ interaction between the depositing monomer and the atoms of the growing island, which corresponds to the leading term in a multipole expansion of the strain energy.[11] In this case they found that the fractal dimension of the growing DLA cluster increased with strain. More recently, the strain dependence of the island density during irreversible submonolayer growth without island relaxation was studied[13,14] using a model in which the elastic interaction was approximated by a $1/r^3$ interaction between all atoms on the surface. In this case the strain was found to lead to an increase in the island-density as well as the critical coverage for nucleation. Earlier, Ratsch *et al.*[15] studied the dependence of the island-size distribution on strain in a reversible model of heteroepitaxial submonolayer growth. However, the effects of strain on the island-shape and scaled island-size distribution in the presence of relaxation have not been studied for the case of irreversible growth. This is of particular interest since in recent work on InAs/GaAs(100) growth, it has been suggested[16] that in the early stages of growth, e.g., before the transition from 2D to 3D islands, the island-size distribution is the same as that for irreversible growth without strain, and thus serves as a template for 3D island formation.

Here we present the results of kinetic Monte Carlo simulations of 2D submonolayer growth with strain for the case of irreversible island growth (corresponding to a critical island size of 1) with rapid island relaxation due to edge- and corner-diffusion. We note that in contrast to previous studies of the effects of strain on the equilibrium island shape,[8–10] the island shape in our model is entirely determined by kinetic factors, and so there is no selected island width as predicted by equilibrium calculations. In addition to studying the island shape, including the scaled island-width and island-length distributions, we also present results for the scaled island-size distribution as a function of strain. Results for the dependence of the island density on deposition flux are also presented.

We note that in our simulations we have approximated the elastic interaction due to strain by an isotropic $1/r^3$ interaction.[12–14] However, unlike Refs. 12–14 in which it has been assumed that the strength of the $1/r^3$ interaction is the same for all adatoms, in most of our simulations we have only included the strain interaction between island atoms, while there is no strain interaction between monomers and other adatoms. This is motivated by the fact that the latter interaction is generally weaker than the interaction between island atoms and may be either attractive or repulsive depending on the system.[17] However, for comparison we have also carried out some simulations in which all adatoms, including both island atoms and monomers, interact with the same $1/r^3$ interaction, and similar results were obtained.

This paper is organized as follows. In Sec. II we first describe the model used and our simulations in more detail. We then present our results for the strain dependence of the

island shape, island-size distribution, island density and scaled island-length and-width distributions in Sec. III. Finally, we summarize our results in Sec. IV.

II. MODEL

In order to study the effects of strain on the island morphology and island-size distribution in irreversible growth, we have carried out kinetic Monte Carlo simulations of a simple model of submonolayer growth which includes irreversible island nucleation as well as rapid island relaxation via edge- and corner-diffusion. In our model, atoms are deposited randomly on a square lattice with deposition rate F and diffuse (hop) to nearest-neighbor sites with diffusion rate D where $D=D_0e^{-E_a/k_BT}$ in the absence of strain. In order to allow for island relaxation, edge diffusion of singly bonded atoms along island edges with rate D_e in the absence of strain, and around corners with rate D_c in the absence of strain, was also included. In most of our simulations we have assumed $D_c=D_e=D$ corresponding to rapid island relaxation. However, for comparison simulations were also carried out with both higher and lower rates of edge- and corner-diffusion. In order to eliminate dimer and trimer diffusion we have suppressed corner rounding for dimers and trimers.

In order to include the effects of strain in our simulations, we have approximated the strain energy by a repulsive $1/r^3$ interaction. We note that a similar approximation has been used in previous work[12,14] and corresponds to the leading term in a multipole expansion of the strain energy.[11] Thus, we may write for the strain energy,

$$E^{st}(\gamma) = \sum_{ij} \frac{\gamma}{r_{ij}^3}, \tag{1}$$

where γ characterizes the strength of the elastic interaction and the sum is over all island adatoms, e.g., all adatoms with one or more nearest-neighbor in-plane bonds. We note that in contrast to previous work[12–14] the interaction due to strain between monomers (corresponding to adatoms with no nearest-neighbor in-plane bonds) and other adatoms is not included since this interaction is in general weaker than the interaction between island atoms and may be either attractive or repulsive depending on the system.[17]

In order to include the effects of strain on the energy barriers for diffusion in our simulations, we have assumed that the shift in the energy barrier for hopping of an atom from site i to site j may be approximated as

$$\Delta E_{ij}^b(\gamma) = \tfrac{1}{2}[E_j^{st}(\gamma) - E_i^{st}(\gamma)], \tag{2}$$

where $E_i^{st}(\gamma)$ is the interaction due to strain between the atom at site i and all other island atoms. This corresponds to an estimate of the strain-induced shift in the saddle-point energy which is a linear interpolation between the corresponding energy shift at the initial site and at the final site. We note that such an interpolation is not exact, since the effect of strain at a saddle-point may be different from that at a binding site.[18,19] However, we expect that it should be a reasonable approximation for the "local" effects of the strain-induced interaction between an island atom and other nearby island atoms.[20] In this connection, we note that in previous work by Fichthorn and Scheffler[21] it has been found that Eq. (2) is a good approximation for the "long-range" interactions between adatoms in Ag on 1 ML Ag/Pt(111) growth. We also note that Eq. (2) implies the existence of an "attachment barrier," due to strain for a monomer to attach to another monomer or an existing island, and also implies a tendency for diffusing edge atoms to diffuse "away" from other island atoms.

Thus, in our model the rate for an atom to hop from site i to a nearest-neighbor or corner diffusion site j is given by

$$D_{ij}(\gamma) = D_{ij}(0)\exp[-(E_j^{st} - E_i^{st})/2k_BT], \tag{3}$$

where $D_{ij}(0)$ is the corresponding rate in the absence of strain. As already noted, in most of our simulations we have assumed $D_{ij}(0)=D_e=D_c=D$. For simplicity, we have also assumed that atoms deposited on top of existing islands do not feel the strain interaction and that there is no barrier to interlayer diffusion at an island edge.

Since the hopping rate of an atom may be different at every lattice site and may also depend on direction, we have used a binary tree[22] to keep track of the rates for all processes and selected kinetic Monte Carlo moves. In our algorithm, the rates for nearest-neighbor and next-nearest-neighbor hops for all sites are stored in the leaves (nodes of the lowest level) of a binary tree. Since the strain energy of an atom depends on its position relative to all other atoms on the substrate, whenever an atom moves its rate has to be recalculated while the rates of all atoms affected by this move also have to be updated. To minimize the computation time only interactions up to a range of 25 lattice units were included during the update after each move. However, periodically the rates for all events in the system were recalculated without any cutoff in order to eliminate any possible accumulation of errors. The interaction of an atom with all of its periodic images was included during this recalculation by the inclusion of precalculated Ewald sums for each possible displacement vector within the lattice.[23]

Our simulations were carried out using a system of size $L=256$ with periodic boundary conditions in both spatial directions, Simulations of submonolayer island growth were carried out using values of D/F ranging from 10^5 to 10^7. Values of the strain energy parameter $\alpha=\gamma/2k_BT$ ranging from $\alpha=0$ (no strain) to $\alpha=2.0$ were used and our results were averaged over 30 runs.

III. RESULTS

A. Monomer and island densities

We first consider the effects of strain on the island and monomer densities. Figure 1 shows a log-log plot of the monomer density N_1 and island density N as a function of coverage θ for $D/F=3\times10^6$ and three different values of the strain parameter α. As can be seen, with increasing strain α both the island and monomer density increase. In addition, the range of the nucleation regime (corresponding to coverages for which the monomer density is larger than the island density) is pushed towards higher coverages with increasing

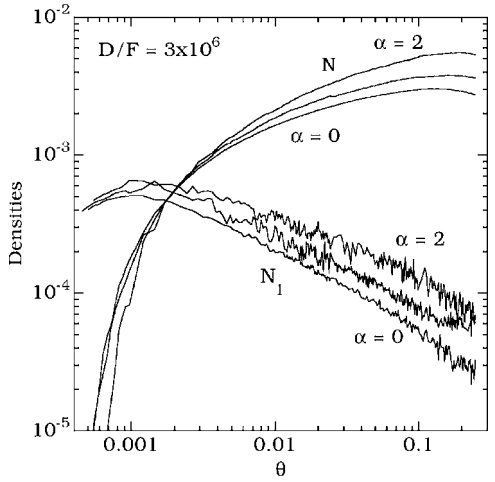

FIG. 1. Monomer density N_1 and island density N as a function of coverage θ with $D/F=3\times10^6$ for $\alpha=0.0$, 1.0, and 2.0.

strain. These effects are primarily due to the strain-induced barrier to dimer formation and are similar to what has been observed in previous simulations of irreversible growth with strain in the absence of island relaxation.[12] Figure 2 shows a plot of the peak island density as a function of D/F for different values of α. As expected, in the absence of strain ($\alpha=0$) the value of χ is close to but slightly lower than $\frac{1}{3}$. However, with increasing strain, the effective value of χ decreases. Again, these results are due primarily to the strain-induced barrier to dimer nucleation and are similar to what has been observed in previous simulations of irreversible growth with strain in the absence of island relaxation.[12]

B. Island morphology

We now consider the effects of strain on the island morphology. Figure 3 shows typical pictures of the island shapes both with and without strain obtained in our simulations for the same parameters as in Fig. 1 ($D/F=3\times10^6$, $\alpha=0-2$). As can be seen, in the absence of strain [Fig. 3(a), $\alpha=0$] but in the presence of relaxation due to edge-and-corner diffusion,

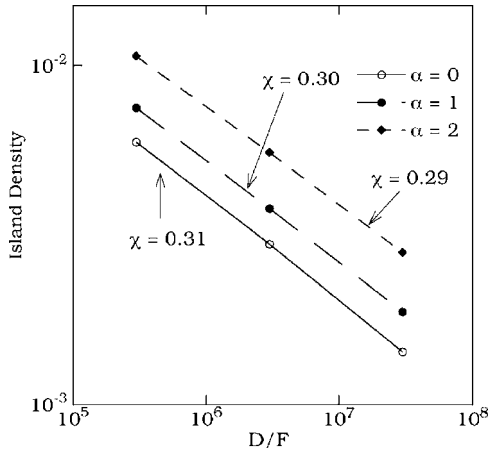

FIG. 2. Peak island density as a function of D/F for $\alpha=0.0$, 1.0 and 2.0.

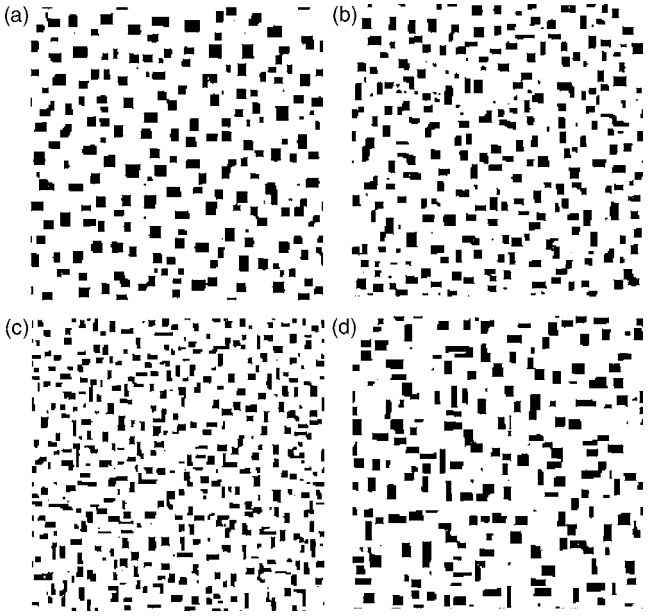

FIG. 3. Island morphology for coverage $\theta=0.2$ with $D/F=3\times10^6$ for strains (a) $\alpha=0.0$, (b) $\alpha=1.0$, (c) $\alpha=2.0$, and (d) $D/F=3\times10^7$ for strain $\alpha=2.0$

square islands are obtained. In contrast, in the presence of sufficient strain, the island size is smaller due to the increased island density while the island shape becomes significantly more rectangular. Also shown in Fig. 3(d) is a picture for a somewhat larger value of D/F (3×10^7) with $\alpha=2$. In this case the average island is somewhat larger than in Fig. 3(c). We also note that while the largest islands tend to be rectangular, the smaller islands are a mixture of square and rectangular islands.

In order to quantify the island morphology we have measured the average aspect ratio $\langle A_r\rangle$, corresponding to the average over all islands of the ratio of the range in the long (x or y) direction to the range in the short direction. Figure 4 shows typical results for the average aspect ratio as a function of strain at coverage $\theta=0.2$ for different values of D/F. As can be seen, the average aspect ratio increases signifi-

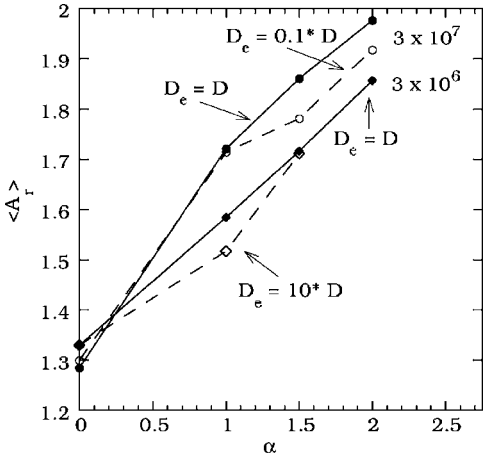

FIG. 4. Average aspect ratio $\langle A_r\rangle$ for $D/F=3\times10^6$ (diamonds) and 3×10^7 (circles) at coverage $\theta=0.2$ as a function of strain α.

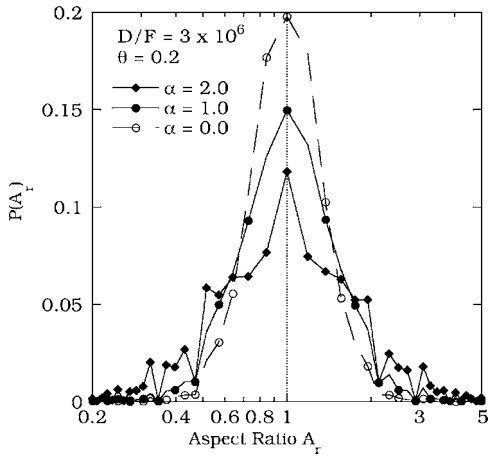

FIG. 5. Aspect ratio distribution $P(A_r)$ for coverage $\theta=0.2$ at $D/F=3\times10^6$ for strains $\alpha=0.0$, 1.0, and 2.0.

cantly with increasing strain. Interestingly, even for the case of zero strain ($\alpha=0$) the average aspect ratio is slightly higher than 1 due to fluctuations. Figure 4 also indicates that, in general, the aspect ratio also increases with increasing D/F for fixed D_e as well as with increasing relaxation rate D_e for fixed D/F for $D_e \leqslant D$. Also shown in Fig. 4 are results for $D_e=10D$ with $D/F=3.0\times10^6$ (open diamonds). As can be seen in this case, due to the very high rate of edge diffusion, the island aspect ratio appears to have saturated, i.e., increasing the rate of edge diffusion does not lead to an increased aspect ratio.

In order to quantify more precisely the island morphology we have also measured the aspect ratio distribution $P(A_r)=N(A_r)/N$ where $N(A_r)$ is the density of islands with aspect ratio A_r and N is the total island density. Figure 5 shows a comparison of the aspect ratio distributions both with and without strain at $\theta=0.2$ with $D/F=3\times10^6$. Due to the equivalence between the x and y directions, both distributions are symmetric about $A_r=1$. We note that even for the case without strain ($\alpha=0$), the aspect ratio distribution has a finite width due to fluctuations. However, with increasing strain the peak at $A_r=1$ decreases significantly while the width of the aspect ratio distribution increases, thus indicating a significant increase in the island anisotropy.

In order to further quantify the island morphology we have also measured the scaled island width and scaled island-length distributions. As already noted, in previous work on the equilibrium island shape for 2D islands[9,10] and 3D islands[8] in the presence of strain, it was found that for islands larger than a critical size, the islands will be rectangular with a selected width which is determined by competition between the surface energy of an island and the strain energy. In contrast, in our nonequilibrium simulations the surface or lateral bond energy does not play a direct role, and as a result fluctuations are likely to be significantly more important.

We first consider the scaled island width distribution, where the island width is defined as the smallest of the lengths corresponding to the range of the island in the x and y directions. Assuming scaling with the average island width W, we may write $N_w(\theta)=A(\theta,W)f_w(w/W)$, where $N_w(\theta)$ is

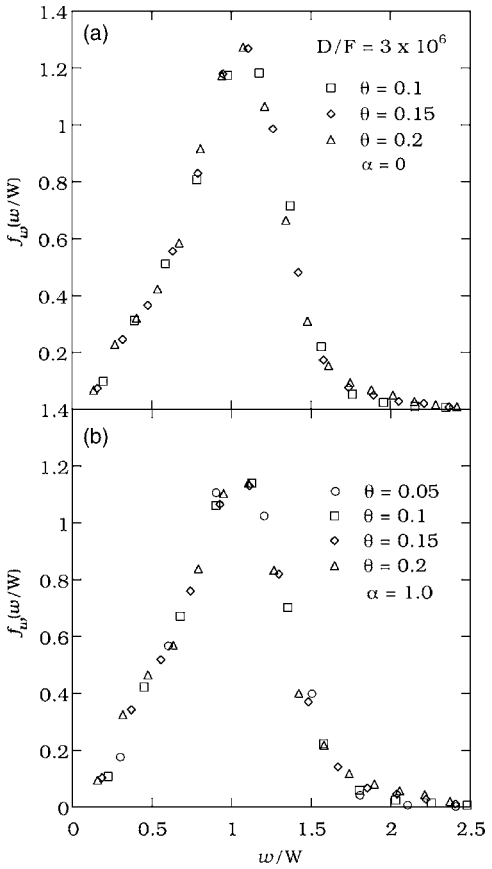

FIG. 6. Scaled island-width distribution $f_w(w/W)$ for different coverages with $D/F=3\times10^6$, (a) $\alpha=0$ and (b) $\alpha=1.0$

the density of islands with width w and $f_w(w/W)$ is the island-width distribution scaling function. Using this definition for the scaling function one may write

$$N_w(\theta)=A(\theta,W)\sum_w f_w(w/W)\simeq AW\int_0^\infty f_w(u)du. \quad (4)$$

Assuming the normalization $\int_0^\infty f_w(u)du=1$ implies $A(\theta,W)=N(\theta)/W$. We thus obtain the general scaling form for the island-width distribution,

$$f_w(w/W)=W\,N_w(\theta)/N(\theta). \quad (5)$$

Figure 6 shows typical results for the scaled island-width distribution $f_w(w/W)$ both with and without strain over a range of coverages up to $\theta=0.2$. As can be seen in both cases there is excellent scaling, i.e., the scaled island-width distribution is independent of coverage. However, in contrast to the predictions of Tersoff and Tromp[8] for the equilibrium island shape, the scaled island-width distribution is relatively broad even in the presence of strain. In addition, the scaled island-width distribution depends only weakly on strain, i.e., the scaled island-width distribution is slightly less sharply peaked in the presence of strain than in the absence of strain.

We have also carried out similar measurements for the scaled island-length distribution. However, in this case we found that the distribution does not scale with the average island length L although it does scale with the peak island

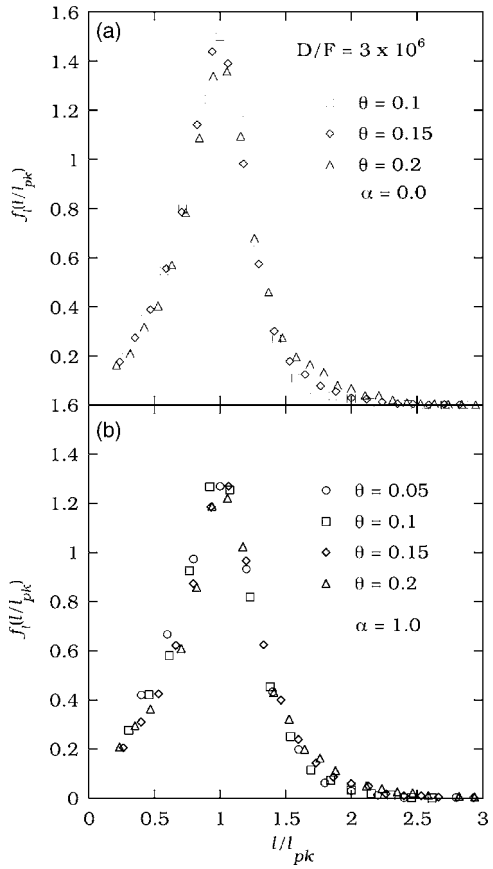

FIG. 7. Scaled island-length distribution $f_l(l/l_{pk})$ for different coverages with $D/F=3\times10^6$, (a) $\alpha=0$ and (b) $\alpha=1.0$

length l_{pk}. Accordingly, one may write for the island-length distribution scaling function

$$f_l(l/l_{pk}) = l_{pk}N_l(\theta)/N(\theta). \tag{6}$$

As shown in Fig. 7, there is again excellent scaling as a function of coverage. However, in this case the peak of the scaled island-length distribution is significantly lower in the presence of strain than in the absence of strain.

C. Island-size distribution

We now consider the effects of strain on the scaled island-size distribution (ISD). This is of particular interest because it has recently been suggested[16] that the 2D island-size distribution in the early stages of heteroepitaxial growth may play an important role in determining the 3D distribution. Figure 8 shows the scaled ISD for the case of large strain ($\alpha=2.0$, $D/F=3\times10^7$) over a range of coverages ranging from 0.05 to 0.2 (solid curve). As can be seen, there is relatively good scaling as a function of coverage. For comparison the scaled ISD in the absence of strain is also included (open symbols) at coverage $\theta=0.1$. As can be seen, there is very little difference between the strained and unstrained results. We note, however, that due to enhanced coalescence the strained ISD has a slightly longer tail than the ISD without strain. In addition, with increasing coverage, the scaled ISD in the presence of strain develops a small peak for small-scaled island size. We attribute this to the delayed nucleation and growth of small islands due to strain.

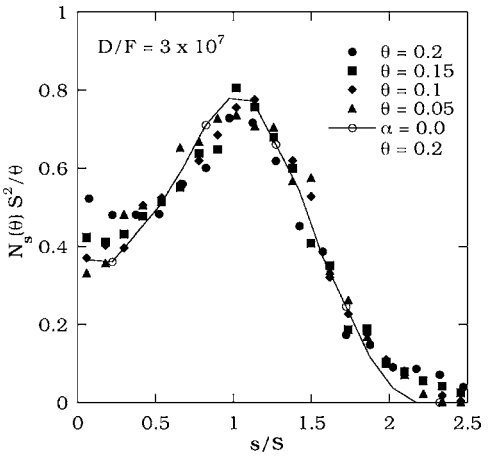

FIG. 8. Scaled island-size distribution with $D/F=3\times10^7$, $\alpha=2.0$, and coverages ranging from $\theta=0.05$ to $\theta=0.2$.

The dependence of the scaled ISD on strain at fixed coverage ($\theta=0.1$) is shown in Fig. 9. As can be seen, there is only a relatively weak dependence of the scaled ISD on strain. We thus conclude that in the case of irreversible growth with fast island relaxation the scaled ISD is only weakly affected by the presence of strain.

IV. CONCLUSION

Using an isotropic $1/r^3$ approximation for the strain interaction, we have studied the effects of strain on the island morphology and size distribution for the case of irreversible island growth with rapid island relaxation. Consistent with previous results obtained in the absence of island relaxation,[13] we find that due to the increase in the barriers to dimer formation and island growth, the nucleation regime increases with increasing strain while the island and monomer densities also increase. However, only a small decrease in the effective island-density scaling exponent χ is observed. Our results also indicate that in the presence of suf-

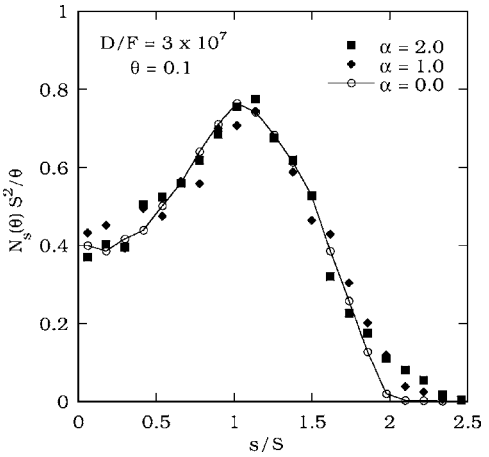

FIG. 9. Scaled island-size distribution with $D/F=3\times10^7$ at coverage $\theta=0.1$ for $\alpha=0$, 1.0, and 2.0.

ficient strain and relaxation due to edge diffusion, the island-shape becomes anisotropic. In particular, the average island aspect ratio $\langle A_r \rangle$ increases approximately linearly with strain. For a fixed strain, the anisotropy also increases with increasing edge diffusion but eventually saturates for large edge diffusion.

In contrast to previous work on the equilibrium island shape in the presence of strain,[8] we find that in the case of irreversible growth with rapid island relaxation, fluctuations play an important role. As a result there is a relatively broad distribution of anisotropies as well as a broad distribution of island widths. We have also derived general scaling forms for the island-width and island-length distributions. In particular, the scaled island-width distribution appears to be independent of coverage and to depend only weakly on strain. For the case of the island length distribution we found that the distribution does not scale with the average island length although it does scale with the peak island length. The resulting scaled island-length distribution is again independent of coverage but depends weakly on the amount of strain.

We have also studied the dependence of the scaled island-size distribution on strain. Somewhat surprisingly, we find that the scaled ISD is only weakly affected by the presence of strain. This is consistent with recent experimental results for the scaled ISD for GaAs/GaAs(001) and InAs/GaAs(001) (Refs. 24 and 25) in which no difference was found between the homoepitaxial and heteroepitaxial cases. We note, however, that in these experiments the resulting scaled ISD is somewhat different from that obtained here due to the anisotropy of the underlying substrate. In the future, it would be interesting to study the effects of strain on the ISD in the case of reversible growth, since in this case the effects of fluctuations are likely to be significantly reduced.

Finally, we note that the values of the strain energy considered in our simulations are quite large compared, for example, to typical strain energies in metal heteroepitaxial growth. As an example, for the case of Cu/Ni(100) submonolayer growth, in which strain relief via island ramification was observed for the case of reversible island growth, a strain interaction energy of approximately 0.015 eV per island atom was estimated[26] which corresponds roughly to $\alpha = \gamma/2k_BT \simeq 0.1$. Since for the values of D/F used in our simulations (see Fig. 4) the island anisotropy is relatively low for this value of α (but increases significantly with D/F), this suggests that in order to observe large island anisotropy due to strain for the case of irreversible growth, relatively large values of D/F are required.

ACKNOWLEDGMENTS

We would like to acknowledge support from the NSF through Grant Nos. DMR-0219328 and CCF-042882 as well as grants of computer time from the Ohio Supercomputer Center (Grant No. PJS0245). We would also like to acknowledge useful discussions with Jerry Tersoff.

[1] Y. Saito, *Statistical Physics of Crystal Growth* (World Scientific, Singapore, 1996).
[2] R. Nötzel, J. Temmyo, and T. Tamamura, Nature (London) **369**, 131 (1994).
[3] R. Jullien, J. Kertesz, P. Meakin, and D. E. Wolf, *Surface Disordering: Growth, Roughening and Phase Transitions* (Nova, Commack, NY, 1993).
[4] M. Notomi, J. Hammersberg, H. Weman, S. Nojima, H. Sugiura, M. Okamoto, T. Tamamura, and M. Potemski, Phys. Rev. B **52**, 11147 (1995).
[5] J. L. Gray, N. Singh, D. M. Elzey, R. Hull, and J. A. Floro, Phys. Rev. Lett. **92**, 135504 (2004).
[6] Y. W. Mo, D. E. Savage, B. S. Swartzentruber, and M. G. Lagally, Phys. Rev. Lett. **65**, 1020 (1990).
[7] D. J. Eaglesham and M. Cerullo, Phys. Rev. Lett. **64**, 1943 (1990).
[8] J. Tersoff and R. M. Tromp, Phys. Rev. Lett. **70**, 2782 (1993).
[9] A. Li, Feng Liu, and M. G. Lagally, Phys. Rev. Lett. **85**, 1922 (2000).
[10] A. Pradhan, N. Y. Ma, and F. Liu, Phys. Rev. B **70**, 193405 (2004).
[11] L. D. Landau and E. M. Lifshitz, *Theory of Elasticity* (Butterworth-Heinemann, Oxford, 1999).
[12] J. Steinbrecher, H. Müller-Krumbhaar, E. A. Brener, C. Misbah, and P. Peyla, Phys. Rev. E **59**, 5600 (1999).
[13] F. Guthiem, H. Müller-Krumbhaar, and E. Brener, Phys. Rev. E **63**, 041603 (2001).
[14] B. M. T. Goncalves and J. F. F. Mendes, Phys. Rev. E **65**, 061602 (2002).
[15] C. Ratsch, A. Zangwill, and P. Šmilauer, Surf. Sci. **314**, L937 (1994).
[16] Y. Chen and J. Washburn, Phys. Rev. Lett. **77**, 4046 (1996).
[17] C. Ratsch, A. P. Seitsonen, and M. Scheffler, Phys. Rev. B **55**, 6750 (1997).
[18] L. Huang, F. Liu, and X. G. Gong, Phys. Rev. B **70**, 155320 (2004).
[19] D. J. Shu, F. Liu, and X. G. Gong, Phys. Rev. B **64**, 245410 (2001).
[20] Here we assume that the effect of strain on the activation barrier for an isolated monomer is already taken into account in the value of D used in our simulations.
[21] K. A. Fichthorn and M. Scheffler, Phys. Rev. Lett. **84**, 5371 (2000).
[22] J. L. Blue, I. Beichl, and F. Sullivan, Phys. Rev. E **51**, R867 (1995).
[23] M. M. Hurley and S. G. Singer, J. Phys. Chem. **96**, 1938 (1992).
[24] V. Bressler-Hill, S. Varma, A. Lorke, B. Z. Nosho, P. M. Petroff, and W. H. Weinberg, Phys. Rev. Lett. **74**, 3209 (1995).
[25] G. R. Bell, T. J. Krzyzewski, P. B. Joyce, and T. S. Jones, Phys. Rev. B **61**, R10551 (2000).
[26] B. Müller, L. P. Nedelmann, B. Fischer, H. Brune, J. V. Barth, K. Kern, D. Erdös, and J. Wollschläger, Surf. Rev. Lett. **5**, 769 (1998).